UAV Swarm-Enabled Localization in Isolated Region: A Rigidity-constrained Deployment Perspective

UAV Swarm-Enabled Localization in Isolated Region: A Rigidity-constrained Deployment Perspective

Qirui Liu, Rongke Liu, *Senior Member, IEEE,* Zijie Wang and John S. Thompson, *Fellow, IEEE*

***Abstract*—In isolated regions, utilizing the unmanned aerial vehicle (UAV) as an aerial anchor node is a promising technique to enable location awareness of ground terminals (GTs). In this letter, considering a UAV swarm-enabled localization for a group of distributed GTs, we aim to minimize the maximum Cramer-Rao lower bound (CRLB) for position estimates with anchor uncertainty. Then, an efficient differential evolution (DE)-based method is proposed to find a sub-optimal solution. In particular, the rigidity of the UAV swarm is recognized as a critical constraint in the problem formulation to provide a unique swarm coordinate configuration and to maintain a prescribed flight formation. A gradient-based local optimization for rigidity is then proposed and embedded in the DE algorithm. Numerical results demonstrate that our proposed designs can reach better performance in localization accuracy while ensuring the rigidity of the UAV swarm, as compared with a random approach.**

***Index Terms*—Unmanned aerial vehicle (UAV) swarm, isolated region, localization, Cramer-Rao lower bound (CRLB), rigidity.**

I. Introduction

LOCALIZATION of ground terminals (GTs) such as mobile phones and wireless sensors has generally been recognized as an enabling technology in various applications (e.g., search and surveillance) [1]. Unfortunately, in some typical isolated regions, positioning signals to GTs from conventional terrestrial base stations (BSs) and satellites are easy to be blocked or severely degraded, making satisfactory localization service no longer available [2], [3]. In this case, unmanned aerial vehicles (UAV) deployed inside the isolated region have the potential to provide a solution for both GTs localization and network services through the air-to-ground (A2G) channel [4], [5]. Research in [6] optimized the UAV trajectory to provide a favorable anchor geometry and reduce the localization error. However, these studies only consider a single UAV with a known precise location, which has limitations in isolated regions. Firstly, the terrestrial networks or the global navigation satellite systems (GNSS) are susceptible to blockage and jamming, which makes it hard to locate the UAV. Moreover, the GTs are served sequentially since the UAV having to move around and communicate with each GT in turn, which may cause severe delay on the time to first fix (TTFF).

These considerations prompt us to consider a UAV swarm-enabled localization system in isolated regions, where the UAVs need to be firstly self-localized to obtain its location information, and then locate the GTs simultaneously. Here range-based network localization can help to locate the UAVs by successive propagation and update of positions from the reference nodes outside the isolated region. In this case, however, utilizing the UAVs as the anchors would inevitably introduce errors in the position estimation of the GTs caused by inaccurate anchor position information [7], which needs to be specifically considered. To further motivate this investigation, we shall focus particularly on the rigidity of the swarming UAVs, which represents a necessary condition for estimating positions using only relative distance measurements and the UAVs' ability to maintain a prescribed formation [8]. For simplicity, we denote the rigidity of the UAV swarm also as swarm rigidity in the following paper. The rigid property is vitally important for the UAV swarm-enabled localization system, since a better self-localization performance provided by the rigidity of the aerial anchors could significantly improve the localization accuracy of the GTs. In a broader context, rigidity is also an important architectural property, which can benefit sensor fusion, exploration and other mission-critical applications of many multi-agent systems [9].

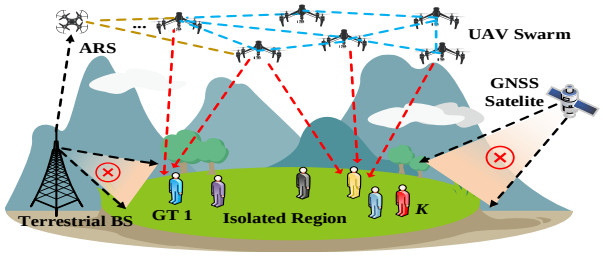

Fig. 1. UAV swarm-enabled localization in an isolated region supports a set $\mathcal{K}$ of GTs.

In this letter, as shown in Fig. 1, we propose a generic analytical framework that includes a UAV swarm to localize a set of GTs simultaneously. Different from the research in [4], [6], the UAVs need to be self-localized before providing localization service, which make the rigid property of the swarm a critical requirement. Therefore, the aim is to minimize the maximum Cramer-Rao lower bound (CRLB) while ensuring the rigidity of the UAV swarm. This design is formulated as an optimization problem of the UAV deployment, which is complicated. In order to find a sub-optimal solution efficiently, this design is solved by a differential evolution (DE)-based method with an embedded local optimization for swarm rigidity. Extensive simulations demonstrate the effectiveness and superiority of the proposed method. To the best of our knowledge, this is the first work to enable simultaneous localization via multiple UAVs under the constraint of rigidity.

This work was supported by the Beijing Municipal Science and Technology Project (Z181100003218008). *(Corresponding author: Rongke Liu.)*

Q. Liu, R. Liu, Z. Wang are with the School of Electronic and Information Engineering and Shenyuan Honors College, Beihang University, Beijing 100191, China (e-mail: {qirui_liu, rongke_liu, wangmajie}@buaa.edu.cn).

J. S. Thompson is with the Institute for Digital Communications, School of Engineering, University of Edinburgh, King's Buildings, Edinburgh, EH9 3JL, U.K. (e-mail: john.thompson@ed.ac.uk).

II. System Model

We consider an isolated region as shown in Fig. 1, where a swarm of N UAVs are employed as aerial anchors to provide time-of-arrival (ToA) localization service for K GTs. ToA localization could achieve relatively high accuracy under line-of-sight (LoS) conditions [10], while the LoS probability generally increases significantly in the A2G channel as the elevation between the aerial anchor and the GT increases [11]. For convenience, we assume the synchronization error could be mitigated with some mature schemes [12]. The locations of GT k and UAV n are denoted by $\mathbf{u}_k = \left[u_x^k, u_y^k, H_G\right]^T \in \mathbb{R}^{3\times 1}, k \in \mathcal{K}$ and $\mathbf{v}_n = \left[v_x^n, v_y^n, H_A\right]^T \in \mathbb{R}^{3\times 1}, n \in \mathcal{V}$. We assume that all GTs and UAVs have the same altitude H_G and H_A, which can be accurately measured with some mature equipment like barometers [13], while our results can be easily extended to a more general case with different altitudes and the corresponding errors. Besides, we assume the UAVs in the swarm and the aerial reference stations (ARS) are both quadrotor platforms and hover at a fixed altitude H_A to provide a relatively stable anchor location during the ranging process.

The operation process of the proposed system is described as the follows. *Preliminaries:* The UAVs/ARS are capable of transmitting/receiving the positioning reference signal (PRS) and the GTs are capable of receiving the PRS, which is a dedicated signal for localization purposes [14]. *Step 1:* By exploiting the PRS for time delay estimation through the air-to-air (A2A) channel [11], range-based self-localization of the UAV swarm is firstly realized by absolute measurements with a set $\mathcal{M}$ of ARS outside the isolated region and relative measurements between the UAVs. *Step 2:* The GT estimates the time delay through the A2G channel [11] using the PRS received from different aerial anchors and then uses a trilateration technique to estimate its position with the location information obtained in *Step 1*.

A. CRLB with Anchor Position Uncertainty

In this subsection, we firstly derive the expression of the anchor position uncertainty introduced by the self-localization of the UAV swarm, which is represented by the lower bound on the error covariance for the unbiased UAV position estimates, and then the CRLB for GT's position estimates with the obtained anchor position uncertainty in *Step 1* is derived.

We denote the Euclidean distance between UAV i and j as $d_{i,j} = \|\mathbf{v}_i - \mathbf{v}_j\|_2$, and we define the effective measurement threshold $\delta_{\text{thr}}^{\text{UAV}}$ to judge whether a range measurement will be included in the observation vector of the UAV self-localization. Here we assume that $\delta_{\text{thr}}^{\text{UAV}}$ can be known a priori based on the UAV transmitting power and the basic requirement of measurement accuracy. If $d_{i,j} \leqslant \delta_{\text{thr}}^{\text{UAV}}$, the corresponding range measurement will be confirmed and included in the observations; otherwise, it will be abandoned. Thus, the associative observation vector of the UAV self-localization $\mathbf{G}(\boldsymbol{\theta}) = \left[\mathbf{d}^{\text{V}}, \mathbf{d}^{\text{R}}\right]^T \in \mathbb{R}^{(G_{\text{V}}+G_{\text{R}})\times 1}$ is formed by stacking the confirmed range measurements, where $\mathbf{d}^{\text{V}} \in \mathbb{R}^{G_{\text{V}}\times 1}$ and $\mathbf{d}^{\text{R}} \in \mathbb{R}^{G_{\text{R}}\times 1}$ denotes the UAV-UAV and UAV-ARS measurements, respectively. In the self-localization of the UAV swarm, the parameter vector of interest consists of the coordinates of the UAVs given by $\boldsymbol{\theta} = \left[v_x^1, v_y^1, \ldots, v_x^N, v_y^N\right]^T \in \mathbb{R}^{2N\times 1}$. According to [15], for any unbiased, non-Bayesian estimator of $\boldsymbol{\theta}$ satisfies

$$\text{Cov}(\hat{\boldsymbol{\theta}}) \succeq \mathbf{F}^{-1}(\boldsymbol{\theta}) = \mathbf{Q}_{\mathcal{V}} \tag{1}$$

where $\text{Cov}(\hat{\boldsymbol{\theta}})$ is the error covariance matrix, and $\mathbf{F}(\boldsymbol{\theta})$ is the Fisher Information Matrix (FIM); the matrix inequality $\text{Cov}(\hat{\boldsymbol{\theta}}) \succeq \mathbf{F}^{-1}(\boldsymbol{\theta})$ denotes that $\text{Cov}(\hat{\boldsymbol{\theta}}) - \mathbf{F}^{-1}(\boldsymbol{\theta})$ is a positive semidefinite matrix, and the CRLB of the UAV self-localization is denoted as $\mathbf{Q}_{\mathcal{V}} \in \mathbb{R}^{2N\times 2N}$. The FIM can be calculated using the standard formula

$$\mathbf{F}(\boldsymbol{\theta}) = \left\{-\mathbb{E}_{\mathbf{G}(\boldsymbol{\theta})|\boldsymbol{\theta}}\left[\nabla_{\boldsymbol{\theta}}(\nabla_{\boldsymbol{\theta}} \ln f\left(\mathbf{G}\left(\boldsymbol{\theta}\right)|\boldsymbol{\theta}\right))^T\right]\right\} \tag{2}$$

where $\mathbb{E}[\cdot]$ denotes the expectation operator; $f\left(\mathbf{G}\left(\boldsymbol{\theta}\right)|\boldsymbol{\theta}\right)$ is the joint probability density function (PDF) of $\mathbf{G}\left(\boldsymbol{\theta}\right)$ parametrized with respect to $\boldsymbol{\theta}$, and $\nabla_{\boldsymbol{\theta}}$ indicates the gradient with respect to $\boldsymbol{\theta}$. For simplicity, we assume the range measurements between the UAVs and ARS through the A2A channel are zero-mean Gaussian distributed with a standard deviation of σ_{A2A}, while the numerical value of σ_{A2A} will be set as a relatively large value relative to the normal A2A channel. The reason of this conservative assumption is that even in hovering state, UAVs would possibly be adversely affected by its own jitter and air flow [16], resulting in a relatively large uncertainty in the range measurements. Therefore, $\mathbf{Q}_{\mathcal{V}}$ can be calculated as

$$\mathbf{Q}_{\mathcal{V}} = \left\{\left(\sigma_{\text{A2A}}^2\right)^{-1}\left[\mathbf{g}\left(\boldsymbol{\theta}\right)\right]^T\left[\mathbf{g}\left(\boldsymbol{\theta}\right)\right]\right\}^{-1} \tag{3}$$

where $\mathbf{g}\left(\boldsymbol{\theta}\right) = \nabla_{\boldsymbol{\theta}}\mathbf{G}\left(\boldsymbol{\theta}\right) \in \mathbb{R}^{(G_{\text{V}}+G_{\text{R}})\times 2N}$ can be recognized as the "pattern" of anchor position uncertainty in the localization of multi-GTs.

The above analysis corresponds to *Step 1* of the proposed system. During the operation of *Step 2*, each GT utilizes L anchors with the largest elevations to minimize the chances of a non-line-of-sight (NLoS) link [1]. The anchor set of GT k is denoted as $\mathcal{V}_k = \{k_1, \ldots, k_L\}, k_l \in \{\mathcal{V}, \mathcal{M}\}$, and its anchor uncertainty matrix $\mathbf{Q}_{\mathcal{V}}^{\mathcal{V}_k}$ is formed by stacking the corresponding elements in (3). Since the ARS are assumed to have precise location knowledge, the mn-th sub-matrix in $\mathbf{Q}_{\mathcal{V}}^{\mathcal{V}_k}$ follows $\boldsymbol{\sigma}_{k_m,k_n}^2 = 0, \exists m, n \in \mathcal{M}$. The range measurement between GT k and anchor k_l is $r_{k,k_l} = d_{k,k_l} + \varepsilon_{k,k_l}, k_l \in \mathcal{V}_k$, where $d_{k,k_l} = \|\mathbf{u}_k - \mathbf{v}_{k_l}\|_2$ is the Euclidean distance and $\varepsilon_{k,k_l} \sim \mathcal{N}(0, \sigma_{k,k_l}^2)$ is the additive noise, and σ_{k,k_l}^2 is calculated according to the bandwidth and signal-to-noise-ratio (SNR) of the received PRS through the A2G channel between the GT and its aerial anchors [6], [14]. Thus, the ranging error covariance matrix is $\mathbf{Q}_{r_k} = \text{diag}(\sigma_{k,k_1}^2, \ldots, \sigma_{k,k_L}^2)$. In this way, the joint likelihood function of the range measurements and the noise-corrupted anchor locations is given by [7]

$$p\left(\mathbf{b}_k \left| \tilde{\mathbf{v}}_{k_1}^T, \ldots, \tilde{\mathbf{v}}_{k_L}^T, \tilde{\mathbf{u}}_k^T\right.\right) = \mathcal{N}\left(\mathbf{b}_k; \boldsymbol{\mu}_k, \mathbf{Q}_k\right) \tag{4}$$

where $\mathbf{b}_k = [r_{k,k_1}, \ldots, r_{k,k_L}, \tilde{\mathbf{v}}_{k_1}^T, \ldots, \tilde{\mathbf{v}}_{k_L}^T]^T \in \mathbb{R}^{3L\times 1}$ stands for the observation vector; $\mathcal{N}\left(\mathbf{b}_k; \boldsymbol{\mu}_k, \mathbf{Q}_k\right)$ denotes the Gaussian density function with the mean $\boldsymbol{\mu}_k$ and covariance $\mathbf{Q}_k$, where $\boldsymbol{\mu}_k = \left[\|\mathbf{u}_k - \mathbf{v}_{k_1}\|_2, \ldots, \|\mathbf{u}_k - \mathbf{v}_{k_L}\|_2, \mathbf{v}_{k_1}^T, \ldots, \mathbf{v}_{k_L}^T\right]^T$ is the noise-free parameter vector; $\mathbf{Q}_k = \text{blkdiag}(\mathbf{Q}_{r_k}, \mathbf{Q}_{\mathcal{V}}^{\mathcal{V}_k})$ and $\text{blkdiag}\left(\cdot\right)$ indicates the block diagonal matrix. Therefore,

the CRLBs for position estimates with anchor uncertainty are given by the diagonal elements of the following matrix

$$\mathbf{CRLB}^k = \left(\mathbf{H}_k^T \mathbf{Q}_k^{-1} \mathbf{H}_k\right)^{-1} \in \mathbb{R}^{(2L+2)\times(2L+2)} \tag{5}$$

where $\mathbf{H}_k = [\mathbf{H}_{r_k}, \mathbf{H}_{\mathcal{V}}^{\mathcal{V}_k}]$ is the Jacobian matrix of the observations; $\mathbf{H}_r \in \mathbb{R}^{L\times(2L+2)}$ and $\mathbf{H}_{\mathcal{V}}^{\mathcal{V}_k} \in \mathbb{R}^{2L\times(2L+2)}$ denote the Jacobian of the range measurements and the anchor positions in $\mathcal{V}_k$, respectively. Finally, the CRLB for the position estimates of GT k is calculated as $\sum_{i=L+1}^{L+2} CRLB_{i,i}^k$, which is the sum of the last two diagonal elements of $\mathbf{CRLB}^k$.

B. Rigidity of the UAV Swarm

In this letter, the *infinitesimally rigid* property is utilized to measure the rigidity of the UAV swarm [8], which is required for maintaining swarm rigidity at all times while operating critical missions in isolated regions [9]. In the study of rigidity, we transform the UAV swarm into a framework $(\mathcal{G}, \mathbf{V})$ to analyze its rigidity-related properties, where $\mathcal{G}=(\mathcal{V}, \mathcal{E})$ represents the corresponding abstract graph; $\mathcal{V}$ is the set of UAV vertices; $\mathcal{E} = \left\{\{i,j\} \,\middle|\, i,j \in \mathcal{V}, d_{i,j} \leqslant \delta_{\text{thr}}^{\text{UAV}}\right\}$ is the edge set generated according to the effective measurement threshold $\delta_{\text{thr}}^{\text{UAV}}$ as introduced in Section II.A, where an effective measurement link in the self-localization process equals to an edge in graph $\mathcal{G}$; vertices i, j are called neighbors $(i \sim j)$ if $\{i,j\} \in \mathcal{E}$; $\mathbf{V}=[\mathbf{v}_1, \ldots, \mathbf{v}_N]^T \in \mathbb{R}^{|\mathcal{V}|\times 2}$ is the coordinates of vertices in $\mathcal{G}$. Then, the edge function $f_{\mathcal{G}} : \mathbb{R}^{2|\mathcal{V}|} \to \mathbb{R}^{|\mathcal{E}|}$ is defined as

$$f_{\mathcal{G}}(\mathbf{V}) = \left(\ldots, \left\|\mathbf{v}_i - \mathbf{v}_j\right\|_2^2, \ldots\right)^T, \{i,j\} \in \mathcal{E}. \tag{6}$$

Using the theorem in the Section III in [8], $(\mathcal{G}, \mathbf{V})$ is *infinitesimally rigid* if and only if $\text{rank}(\dot{f}_{\mathcal{G}}) = 2|\mathcal{V}| - 3$, where $\dot{f}_{\mathcal{G}}$ is defined as the rigidity matrix $\mathbf{R}_{\mathcal{G}}(\mathbf{V}) \doteq \partial f_{\mathcal{G}}(\mathbf{V}) / \partial \mathbf{V} \in \mathbb{R}^{|\mathcal{E}|\times 2|\mathcal{V}|}$. Research in [9] further extended the above rank condition in terms of the eigenvalues of a symmetric and positive semidefinite matrix $\mathcal{R}_{\mathcal{G}} \doteq \mathbf{R}_{\mathcal{G}}(\mathbf{V})^T \mathbf{R}_{\mathcal{G}}(\mathbf{V}) \in \mathbb{R}^{2|\mathcal{V}|\times 2|\mathcal{V}|}$ with a immediate consequence: $\text{rank}(\mathbf{R}_{\mathcal{G}}(\mathbf{V})) = \text{rank}(\mathcal{R}_{\mathcal{G}})$. The eigenvalues of $\mathcal{R}_{\mathcal{G}}$ are denoted as $\lambda_1 \leqslant \lambda_2 \leqslant \ldots \leqslant \lambda_{2|\mathcal{V}|}$, and the *infinitesimal rigidity* of $(\mathcal{G}, \mathbf{V})$ is equivalent to $\lambda_1 = \lambda_2 = \lambda_3 = 0$ and $\lambda_4 > 0$. Therefore, λ_4 becomes a effective measure of *infinitesimal rigidity*, i.e., the *rigidity eigenvalue*, which can be expressed as

$$\begin{aligned}\lambda_4 = \boldsymbol{\alpha}_4^T \mathcal{R}_{\mathcal{G}} \boldsymbol{\alpha}_4 = \sum_{i\sim j} \Big[&\left(v_x^i - v_x^j\right)^2 \left(\alpha_x^i - \alpha_x^j\right)^2 + \\ &\left(v_y^i - v_y^j\right)^2 \left(\alpha_y^i - \alpha_y^j\right)^2 + \\ &2\left(v_x^i - v_x^j\right)\left(v_y^i - v_y^j\right)\left(\alpha_x^i - \alpha_x^j\right)\left(\alpha_y^i - \alpha_y^j\right)\Big]\end{aligned} \tag{7}$$

where $\boldsymbol{\alpha}_4 = \left[\alpha_x^T, \alpha_y^T\right]^T$ is the normalized *rigidity eigenvector* associated with λ_4.

III. Problem Formulation

In this letter, we aim to minimize the maximum CRLB of GTs by optimizing the UAV swarm deployment. Furthermore, to provide the fundamental ability to control the swarm formation, swarm rigidity is also recognized as a critical constraint. Thus, the problem of interest is formulated as

$$(\text{P1}): \min_{\mathbf{V}} \max_{k\in\mathcal{K}} \sum_{i=L+1}^{L+2} CRLB_{i,i}^k \tag{8}$$

$$\text{s.t. C1: } v_{\min} \leqslant v_{x,y}^i \leqslant v_{\max}, \forall i \in \mathcal{V} \tag{9}$$

$$\text{C2: } \left\|\mathbf{v}_i - \mathbf{v}_j\right\| \leqslant \delta_{\text{thr}}^{\text{UAV}}, \forall \{i,j\} \in \mathcal{E} \tag{10}$$

$$\text{C3: } \left\|\mathbf{v}_i - \mathbf{v}_j\right\| \geqslant \delta_{\text{thr}}^{\text{safe}}, \forall i,j \in \mathcal{V} \tag{11}$$

$$\text{C4: } \lambda_4(\mathbf{V}) \geqslant \lambda_{\text{thr}}^{\text{rigid}} \tag{12}$$

where $\mathcal{G}=(\mathcal{V}, \mathcal{E})$ is the corresponding graph of $\mathbf{V}$; $v_{\min}$ and $v_{\max}$ are the boundaries of the UAV deployment; $\delta_{\text{thr}}^{\text{UAV}}$ is the maximum effective measurement range for the UAVs; $\delta_{\text{thr}}^{\text{safe}}$ denotes the minimum distance between UAVs for safety reasons; $\lambda_{\text{thr}}^{\text{rigid}} > 0$ is the minimum threshold for the rigidity eigenvalue $\lambda_4(\mathbf{V})$ to prevent the swarm becoming *infinitesimally flexible*, which is the opposite state to the desired *infinitesimally rigid* condition, causing ambiguity in the network localization and posing a threat to formation control [9].

IV. Proposed Method

Problem (P1) is a non-convex problem, and there is no closed-form expression for the CRLB in the objective function, which makes this problem complicated. Differential evolution (DE) has generally been recognized as one of the most powerful derivative-free optimization algorithms in current use, which is suitable for solving this problem [6], [17]. Therefore, a DE-based optimization method is proposed to obtain an efficient sub-optimal solution. In our proposed DE-based method, the a-th individual in the l-th iteration represents the UAV swarm deployment $\mathbf{V}_{l,a} \in \mathbb{R}^{|\mathcal{V}|\times 2}$. According to problem (P1), the fitness function used for evaluating the individual solutions is defined as

$$\text{fit}(\mathbf{V}_{l,a}) = \left(\alpha_{\text{Loc}}\beta_{\text{Loc}} + \alpha_{\text{Safe}}\beta_{\text{Safe}} + \alpha_{\text{Rig}}\beta_{\text{Rig}}\right)^{-1} \tag{13}$$

where β_{Loc} is the maximum CRLB of the GTs corresponding to $\mathbf{V}_{l,a}$; β_{Safe} and β_{Rig} are the penalty terms of C3 and C4, respectively. Once $\mathbf{V}_{l,a}$ fails to guarantee the safety and rigidity constraint of the swarm, we set $\beta_{\text{Safe}} = 1$ and $\beta_{\text{Rig}} = 1$, otherwise, both values are set to zero. The values of weights α_{Safe} and α_{Rig} should be much larger than that of $\alpha_{\text{Loc}}\beta_{\text{Loc}}$ to punish an unfeasible solution, which will be eliminated during the iterations. Note that constraint (9) and (10) will be satisfied when generating individuals and calculating the CRLB and the rigidity eigenvalue, respectively. The proposed DE-based optimization method is shown in Algorithm 1.

It should be noted that an individual $\mathbf{V}_{l,a}$ with a good CRLB may be punished by a very low fitness value and eliminated during the iterations if $\lambda_4(\mathbf{V}_{l,a})$ is a little bit lower than the rigidity threshold $\lambda_{\text{thr}}^{\text{rigid}}$, which is a harsh criterion. Thus, we design a local optimization of swarm rigidity for each individual to improve $\lambda_4(\mathbf{V}_{l,a})$ before the calculation of the fitness value and the selection operation of the DE algorithm, as shown in steps 5-6 in Algorithm 1. The proposed local optimization method is summarized in Algorithm 2. Here we aim to find a local optimal solution of the *rigidity eigenvalue* near $\mathbf{V}_{l,a}$ using its gradient with respect to the UAVs' locations, which is calculated as

$$\begin{aligned}\frac{\partial \lambda_4(\mathbf{V}_{l,a})}{\partial v_{x,l,a}^i} = 2\sum_{i\sim j} \Big(&\left(v_{x,l,a}^i - v_{x,l,a}^j\right)\left(\alpha_{x,l,a}^i - \alpha_{x,l,a}^j\right)^2 + \\ &\left(v_{y,l,a}^i - v_{y,l,a}^j\right)\left(\alpha_{x,l,a}^i - \alpha_{x,l,a}^j\right)\left(\alpha_{y,l,a}^i - \alpha_{y,l,a}^j\right)\Big)\end{aligned} \tag{14}$$

Algorithm 1 Proposed DE-Based Optimization Method

Input: Number of individuals N_p, maximal iterations $l_{\max}$.
Output: Optimal UAV swarm deployment $\mathbf{V}^*$.

1: Randomly generate initial population $\mathbf{P}_0 \triangleq \{\mathbf{V}_{0,1},\ldots,\mathbf{V}_{0,N_p}\}$.
2: **for** $l=0; l<l_{\max}; l=l+1$ **do**
3: Calculate the fitness of the individuals in $\mathbf{P}_l$ using (13);
4: Generate a temporary population $\dot{\mathbf{P}}_l \triangleq \{\dot{\mathbf{V}}_{l,1},\ldots,\dot{\mathbf{V}}_{l,N_p}\}$ according to the *mutation* and *crossover* processes of the DE algorithm [6];
5: Find the local optimal swarm rigidity for each individual in $\dot{\mathbf{P}}_l$ using ***Algorithm 2***, and the obtained local optimal solution $\ddot{\mathbf{P}}_l$ is regarded as the trial population;
6: Calculate the fitness of the individuals in $\ddot{\mathbf{P}}_l$ using (13);
7: Generate a new population $\mathbf{P}_{l+1}$ from $\mathbf{P}_l$ and $\ddot{\mathbf{P}}_l$ with the *selection* process in the DE algorithm [6];
8: Select the optimal solution $\mathbf{V}^*=\mathbf{V}_{l+1,i^*}$, where $i^* = \underset{i\in\{1,\ldots,N_p\}}{\arg\max}\ \text{fit}(\mathbf{V}_{l+1,i})$;
9: **end for**

Algorithm 2 Local Optimization for Swarm Rigidity

Input: Rigidity threshold $\lambda_{\text{thr}}^{\text{rigid}}$, step size Δt, tolerance $\kappa_2 \gg \kappa_1 > 0$, $\dot{\mathbf{P}}_l$ generated in the step 4 of ***Algorithm 1***.
Output: Local optimal solution $\ddot{\mathbf{P}}_l$ for swarm rigidity.

1: **for** each $\dot{\mathbf{V}}_{l,a} \in \dot{\mathbf{P}}_l$ **do**
2: **if** $0 < \lambda_4(\dot{\mathbf{V}}_{l,a}(\mathcal{G},p)) < \lambda_{\text{thr}}^{\text{rigid}}$ **then**
3: **for** $c=0; c<c_{\max} \& |\Delta\lambda_4| \geqslant \kappa_1; c=c+1$ **do**
4: Optimize $\lambda_4(\mathbf{V}_{l,a})$ with its gradient: $\dot{\mathbf{V}}_{l,a}^{c+1} = \dot{\mathbf{V}}_{l,a}^{c} - \Delta t \cdot (\partial\lambda_4(\dot{\mathbf{V}}_{l,a}^{c})/\partial\dot{\mathbf{V}}_{l,a}^{c})$;
5: Calculate the fractional increase of the rigidity eigenvalue $\Delta\lambda = \lambda_4(\dot{\mathbf{V}}_{l,a}^{c+1}) - \lambda_4(\dot{\mathbf{V}}_{l,a}^{c})$;
6: **if** $\Delta\lambda < -\kappa_2$ **then**
7: Return to the previous solution $\dot{\mathbf{V}}_{l,a}^{c}$ and **break**;
8: **end if**
9: **end for**
10: $\ddot{\mathbf{V}}_{l,a} \leftarrow \dot{\mathbf{V}}_{l,a}^{c_{break}}, \ddot{\mathbf{P}}_l = \{\ddot{\mathbf{V}}_{l,1},\ldots,\ddot{\mathbf{V}}_{l,a}\}$
11: **else**
12: $\ddot{\mathbf{V}}_{l,a} \leftarrow \dot{\mathbf{V}}_{l,a}, \ddot{\mathbf{P}}_l = \{\ddot{\mathbf{V}}_{l,1},\ldots,\ddot{\mathbf{V}}_{l,a}\}$
13: **end if**
14: **end for**

$$\frac{\partial\lambda_4(\mathbf{V}_{l,a})}{\partial v_{y,l,a}^i} = 2\sum_{i\sim j}\Big((v_{y,l,a}^i - v_{y,l,a}^j)(\alpha_{y,l,a}^i - \alpha_{y,l,a}^j)^2 + (v_{x,l,a}^i - v_{x,l,a}^j)(\alpha_{x,l,a}^i - \alpha_{x,l,a}^j)(\alpha_{y,l,a}^i - \alpha_{y,l,a}^j)\Big). \quad (15)$$

In particular, the optimization of the *rigidity eigenvalue* may cause the creation or disconnection of measurement links in $(\mathcal{G},\mathbf{V})$ due to the the maximum effective measurement threshold $\delta_{\text{thr}}^{\text{UAV}}$. Hence, there should be an insurance strategy to avoid a sharp deterioration of the swarm rigidity, which is summarized in steps 6-8 of Algorithm 2.

V. Simulation Results and Discussion

In this section, a series of numerical simulations are conducted to evaluate the validity and performance of the proposed design. We consider a system with $N=|\mathcal{V}|=15$ UAVs, $M=6$ ARS, and $K=10$ GTs located in an isolated circular region where the radius is 800m and the center is the origin $(0,0,0)$. The ARS are evenly distributed on the circumference with a radius of 1km and remain stationary during the optimization of the UAV deployment. The bandwidth is 10MHz and the main frequency is 2.4GHz, where ideal muting is considered for the interference modeling [14]. The transmit power of the UAV is 23dBm. The additive white Gaussian noise (AWGN) power spectral density $N_0 = -174$dBm/Hz, and the noise figure of the GTs is set as 9dB. The number of anchors associated with each GT $L=5$ and the parameters of the proposed method are: $N_p=10$, $l_{\max}=100$, $\alpha_{\text{Loc}}=1$, $\alpha_{\text{Safe}}=\alpha_{\text{Rig}}=10$, $c_{\max}=30$, $\kappa_1=$ 1e3, $\kappa_2=$ 1e4, and $\Delta t=0.1$. Furthermore, we set $\delta_{\text{thr}}^{\text{UAV}}=800$m, $\delta_{\text{thr}}^{\text{safe}}=100$m, $\lambda_{\text{thr}}^{\text{rigid}}=$ 2e5, $H_G=1.5$m, $H_A=200$m, $v_{\max}=-v_{min}=800$ and $\sigma_{\text{A2A}}=5$m. The results obtained are based on one random realization of the GT locations as shown in Fig. 2(c). Fig. 2(a) demonstrates the effects of using the proposed DE-based method in Algorithm 1, where the best (i.e., the minimum) and the average localization error $\sigma(\mathbf{V}) = \sqrt{\sum_{i=L+1}^{L+2} CRLB_{i,i}^k}$ in meter (m) of N_p individuals in the population decrease constantly as the iteration number increases. The final optimized UAV deployment $\mathbf{V}^*$ improves the localization accuracy of the proposed system by about 44.3% compared with the best individual $\mathbf{V}_{0,\text{best}}$ in the unoptimized random population $\mathbf{P}_0$. An application example of the proposed local optimization method for swarm rigidity in Algorithm 2 is shown in Fig. 2(b), where the swarm rigidity of a single individual is better satisfied when it equals 5.06e5 rather than 1.78e5 following the gradient of the *rigidity eigenvalue* in (7). The optimized UAV deployment $\mathbf{V}^*$ obtained by the proposed method is also shown in Fig. 2(c), where the maximum localization error of the GTs is 2.52m, and the minimum distance between the UAVs is 142.35m, while $\lambda_4(\mathbf{V}^*)=3.80$e5.

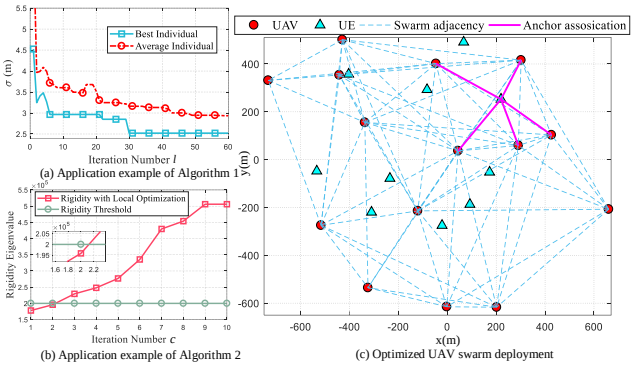

Fig. 2. Application examples of the proposed methods and corresponding optimization results.

It should be noted that Fig. 2 shows an application example for a single simulation run. In order to make a statistical evaluation of the proposed design, 100 Monte-Carlo simulations are implemented, and the results obtained are shown in Fig. 3 and Fig. 4. In this letter, the benchmark comparison is selected as a random approach according to some specific constraints, which is a common strategy in anchor deployment [18]. Specifically, a solution $\mathbf{V}_{random}$ generated with the random approach follows three constraints: 1) the relaxed rigidity constraint $\lambda_4(\mathbf{V}_{random}) > 0$; 2) the availability of localization $\sigma(\mathbf{V}_{Random}) < +\infty$; 3) the boundaries of the

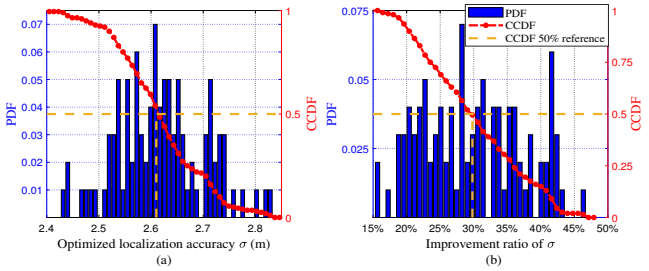

Fig. 3. Statistical results: (a) the localization accuracy of the optimized solutions using the proposed DE-based method, and (b) the improvement ratio of the localization accuracy compared with the random benchmark approach.

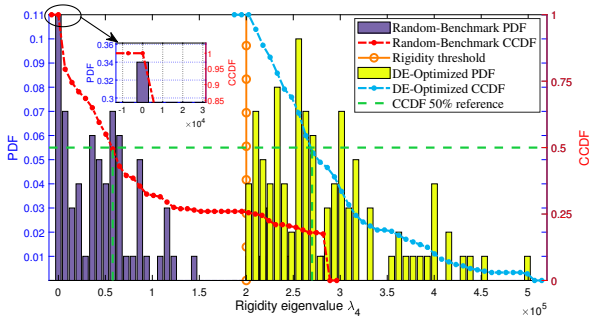

Fig. 4. Statistical results: the rigidity eigenvalue of the solutions realized by 1) the random benchmark approach and 2) the proposed DE-based method.

UAV deployment, which is the same setting as C1 in problem (P1). Here, we compare the optimal solution of each Monte Carlo simulation of the proposed DE-based method and the random benchmark method. The probability density function (PDF) of the localization error $\sigma(\mathbf{V}^*)$ obtained by the proposed DE-based method and the improvement relative to the benchmark method are shown in Fig. 3(a) and (b), where the improvement ranges from 15.7% to 46.3%. The PDFs of the corresponding rigidity eigenvalues $\lambda_4(\mathbf{V}_{random})$ and $\lambda_4(\mathbf{V}^*)$ are shown in Fig. 4, where all values of $\lambda_4(\mathbf{V}_{random})$ are larger than the pre-defined rigidity threshold $\lambda_{\text{thr}}^{\text{rigid}}$. However, the rigidity eigenvalues of the benchmark approach demonstrated by the purple bars are relatively small, where only 25% of them have reached $\lambda_{\text{thr}}^{\text{rigid}}$, and 34% of them are nearly zero. The complementary cumulative distribution functions (CCDF) are demonstrated by dash-dotted lines in Fig. 3 and 4, which can be interpreted as: the probability of increasing the location accuracy by more than 29.8% is 50%, and half of the corresponding rigidity eigenvalues are larger than 2.61e5.

VI. Conclusion

This letter proposes a generic analytical framework for UAV swarm-enabled localization in isolated regions from a rigidity-constrained deployment optimization perspective, where the UAVs have a mission of locating the GTs while maintaining a target quality-of-rigidity for formation control. Specifically, we formulated the deployment optimization problem to minimize the maximum CRLB, subject to a minimum rigidity constraint. We proposed a DE-based method with a local optimization of the swarm rigidity for finding a sub-optimal solution efficiently. Numerical results demonstrate the feasibility of our design and the proposed optimization method could further improve the localization accuracy by around 30% compared with a random approach. Consequently, we foresee that the UAV is likely to play a critical role in future localization system and especially in isolated regions.

References

[1] H. Sallouha, M. M. Azari, A. Chiumento, and S. Pollin, "Aerial anchors positioning for reliable RSS-based outdoor localization in urban environments," *IEEE Wireless Communications Letters*, vol. 7, no. 3, pp. 376–379, 2018.

[2] C. Zhan, Y. Zeng, and R. Zhang, "Energy-efficient data collection in UAV enabled wireless sensor network," *IEEE Wireless Communications Letters*, vol. 7, no. 3, pp. 328–331, 2018.

[3] X. Wang, H. Zhang, and V. C. M. Leung, "Modeling and performance analysis of UAV-assisted cellular networks in isolated regions," in *2018 IEEE International Conference on Communications Workshops (ICC Workshops)*, 2018, pp. 1–6.

[4] H. Sallouha, M. M. Azari, and S. Pollin, "Energy-constrained uav trajectory design for ground node localization," in *2018 IEEE Global Communications Conference (GLOBECOM)*, 2018, pp. 1–7.

[5] S. Zhang, Y. Zeng, and R. Zhang, "Cellular-enabled UAV communication: A connectivity-constrained trajectory optimization perspective," *IEEE Transactions on Communications*, vol. 67, no. 3, pp. 2580–2604, 2019.

[6] Z. Wang, R. Liu, Q. Liu, J. S. Thompson, and M. Kadoch, "Energy-efficient data collection and device positioning in UAV-assisted IoT," *IEEE Internet of Things Journal*, vol. 7, no. 2, pp. 1122–1139, 2020.

[7] F. K. W. Chan and H. C. So, "Accurate distributed range-based positioning algorithm for wireless sensor networks," *IEEE Transactions on Signal Processing*, vol. 57, no. 10, pp. 4100–4105, 2009.

[8] L. Asimow and B. Roth, "The rigidity of graphs II," *Journal of Mathematical Analysis and Applications*, vol. 68, no. 1, pp. 171–190, 1979.

[9] D. Zelazo, A. Franchi, F. Allgöwer, H. Bülthoff, and P. R. Giordano, *Rigidity Maintenance Control for Multi-Robot Systems-Robotics: Science and Systems VIII*. MIT Press, 2013.

[10] F. K. W. Chan and H. C. So, "Accurate distributed range-based positioning algorithm for wireless sensor networks," *IEEE Transactions on Signal Processing*, vol. 57, no. 10, pp. 4100–4105, 2009.

[11] W. Khawaja, I. Guvenc, D. W. Matolak, U. Fiebig, and N. Schneckenburger, "A survey of air-to-ground propagation channel modeling for unmanned aerial vehicles," *IEEE Communications Surveys Tutorials*, vol. 21, no. 3, pp. 2361–2391, 2019.

[12] B. J. Choi, H. Liang, X. Shen, and W. Zhuang, "DCS: Distributed asynchronous clock synchronization in delay tolerant networks," *IEEE Transactions on Parallel and Distributed Systems*, vol. 23, no. 3, pp. 491–504, 2012.

[13] J. Rantanen, L. Ruotsalainen, M. Kirkko-Jaakkola, and M. Mäkelä, "Height measurement in seamless indoor/outdoor infrastructure-free navigation," *IEEE Transactions on Instrumentation and Measurement*, vol. 68, no. 4, pp. 1199–1209, 2019.

[14] J. A. del Peral-Rosado, J. A. López-Salcedo, G. Seco-Granados, F. Zanier, and M. Crisci, "Achievable localization accuracy of the positioning reference signal of 3GPP LTE," in *2012 International Conference on Localization and GNSS (ICL-GNSS)*, 2012, pp. 1–6.

[15] M. Angjelichinoski, D. Denkovski, V. Atanasovski, and L. Gavrilovska, "Cramér–rao lower bounds of RSS-based localization with anchor position uncertainty," *IEEE Transactions on Information Theory*, vol. 61, no. 5, pp. 2807–2834, 2015.

[16] D. Xu, Y. Sun, D. W. K. Ng, and R. Schober, "Multiuser MISO UAV communications in uncertain environments with no-fly zones: Robust trajectory and resource allocation design," *IEEE Transactions on Communications*, vol. 68, no. 5, pp. 3153–3172, 2020.

[17] S. Das and P. N. Suganthan, "Differential evolution: A survey of the state-of-the-art," *IEEE Transactions on Evolutionary Computation*, vol. 15, no. 1, pp. 4–31, 2011.

[18] S. Büyükçorak, G. K. Kurt, and A. Yongaçoğlu, "UAV assisted ground user localization," in *2019 IEEE International Conference on Wireless for Space and Extreme Environments (WiSEE)*, 2019, pp. 111–115.